Crossover from the hydrodynamic regime to the thermal fluctuation regime in a two-dimensional phase-separating binary fluid containing surfactants

Jiunn-Ren Roan* and Chin-Kun Hu†
Institute of Physics, Academia Sinica, Nankang, Taipei 115, Taiwan
(Received 10 September 1999; revised manuscript received 20 December 1999)

Extensive simulations were carried out to investigate the crossover between the hydrodynamic regime at intermediate stage and the thermal fluctuation regime at late stage in a phase-separating binary fluid/surfactant system in two dimensions. The existence of the crossover and its dependence on the surfactant concentration were analyzed using Kawasaki and Ohta's interface kinetic equation [Physica A **118**, 175 (1983)]. The analysis showed that there should exist a critical surfactant concentration, above which thermal fluctuations dominate phase separation at all times. Simulations suggested that the crossover exists and the hydrodynamic regime shrinks when surfactant concentration increases. Simulations also demonstrated that the trapped surfactants seen in a previous study [Phys. Rev. E **59**, 2109 (1999)] can remain trapped for a time much longer than the time needed to form well segregated domains, in spite of the presence of significant thermal fluctuations.

PACS number(s): 05.70.Fh, 82.70.Kj, 64.75.+g

I. INTRODUCTION

One of the major concerns in the numerical study of phase separation of fluids lies in the examination and confirmation of the dynamic scaling hypothesis and the determination of the growth exponent that describes the growth of the average domain size [1]. The hypothesis has been confirmed in many numerical studies of various systems and the growth exponent determined usually is consistent with theoretical predictions. The exponent is known to depend on many factors. Dimensionality, viscosity, and inertial effects are among the better known factors that affect the value of the exponent [1]. Depending on the relative importance of these factors, there can exist crossovers at which the growth exponent changes from one value to another [2]. Less is known about the effects of impurities [3], surfactants [4–6], and boundary conditions [7] on the dynamic scaling hypothesis, growth exponents, and associated crossovers.

When the binary fluid contains a third component such as impurities or surfactants, its phase separation kinetics becomes more complicated. Many researchers have attempted to determine the growth exponent. Scaling laws that are more sophisticated than the simple algebraic scaling seen in the pure binary fluid have also been proposed. For the case of binary fluid/surfactant, it is unclear whether dynamic scaling holds and, if it holds, what are the growth exponents in different regimes. To determine the growth exponent usually one examines the growth of the average domain size R as a function of time (more precisely, the number of time steps) and fits the data according to a presumed scaling form such as $R(t)\sim t^{\alpha}$ or $R(t)\sim(\log t)^{\alpha}$. When the presumed scaling law can fit the data reasonably well over a sufficiently wide range of time, it is tempting to conclude that the growth follows the proposed growth law and the growth exponent is given by the optimal α. In a previous study by one of us this procedure was questioned [8]. The system examined in Ref. [8] does not exhibit dynamical scaling. Nevertheless, it was found that the domain growth could be fitted by $R(t)\sim t^{\alpha}$ and $R(t)\sim(\log t)^{\alpha}$ equally well even when dynamical scaling does not hold. This fact prompted one of us to examine the validity of fitting data using simple scaling forms. It was argued that, even when dynamic scaling truly holds, namely, even when a single length scale dominates the system, the scaling of this length scale in a binary fluid/surfactant system can still be far more complicated than what a simple data fitting can encompass [9]. The argument was based on a very general kinetic equation derived by Kawasaki and Ohta [10]. We believe that any model for the binary fluid/surfactant system that is based on the time-dependent Ginzburg-Landau approach [11] falls within the range of this kinetic equation and the argument in Ref. [8] applies. Accordingly, trying to hypothesize simple scaling forms and determine their associated growth exponents in a complicated system such as a binary fluid containing surfactants very likely will lead to disagreement between simulations, as seen in the literature. Hence, for complicated system such as binary fluid/surfactants, it may not be meaningful to debate which hypothetical scaling law gives the best description and to determine the corresponding growth exponents.

However, regardless whether the dynamic scaling holds or not in systems more complicated than binary fluids, it is still meaningful, as it is for binary fluids, to investigate the possible crossovers in the binary fluid/surfactant system. We know for certain that, whether the dynamic scaling or simple hypothetical scaling laws hold or not, a binary fluid containing surfactant should gradually approach a stationary state in which the average domain size is largely determined by the surfactant concentration. Thermal fluctuations presumably dominate this regime. On the other hand, when the surfactant concentration approaches zero, a binary fluid/surfactant system reduces to a binary fluid, so hydrodynamics should resume its dominance in phase separation, as it does in pure binary fluids. Therefore, there should exist a crossover at which the main driving force of the phase separation changes

*Present address: Doi Project, Nagoya University, Research & Education Center 1-4F, Furo-cho, Chikusa-ku, Nagoya, 464-8601, Japan. Electronic address: roan@post.harvard.edu
†Electronic address: huck@phys.sinica.edu.tw

from hydrodynamics to thermal fluctuations. When the crossover will set in apparently depends on the amount of surfactant in the system. One of the purposes of this paper is to investigate the existence of this crossover, its sharpness, and its dependence on the surfactant concentration.

Most numerical studies on the phase separation kinetics of binary fluid/surfactant systems ignore hydrodynamic effects in order to render the simulations more computationally economic. It is, however, paradoxical to study a complex fluid without considering its fluid nature. Attempts to include hydrodynamics exist, but within the Ginzburg-Landau approach [11], Refs. [12] and [8] are probably the only simulations that include hydrodynamic effects. An interesting phenomenon observed when hydrodynamics is included is the trapping of surfactants in the domains of the binary fluid [8]. This phenomenon can be easily explained in terms of the equation of motion for surfactants and, although the same reasoning also applies when hydrodynamics is not included, simulations show that only with the assistance of hydrodynamic convection can the domain walls move fast enough to trap the surfactants [8]. It is natural to suspect that the surfactants are just temporarily trapped and thermal fluctuations, if included, will eventually help them migrate to the interfaces between fluid domains. To examine this, Ref. [8] attempted a preliminary simulation that included diffusion, hydrodynamics, and thermal fluctuations [13]. However, although the thermal fluctuations were tuned to their maximum strength within the stability range of the simulation, the simulation time covered (5×10^5 time steps) was too short. Another purpose of this paper therefore is to perform more extensive simulations, to 2.5×10^6 time steps, to assess the lifetime of the trapped surfactants.

This paper is organized as follows. Section II briefly describes the model and method used in simulations. Readers are referred to Refs. [8] and [14] for more details. Section III A discusses the results. There it is shown first theoretically that the crossover should exist and how it will depend on the surfactant concentration. This analysis is then compared with simulations. The crossover from the hydrodynamic to the thermal fluctuation regime observed in simulations can be located by two methods. The dependence of the crossover location on the surfactant concentration is analyzed. It also shows how changes in temperature and fluidity affect the crossover. Section III B shows that the trapping of surfactants seen in Ref. [8] can persist for an extremely long time. The implication of this long lifetime is discussed. Section IV concludes the finding of this paper.

II. MODEL AND SIMULATION METHOD

Consider a mixture of binary fluid and surfactant. Let $\psi(\mathbf{r},t)$ be the concentration difference between the two components of the binary fluid and $\rho(\mathbf{r},t)$ the surfactant concentration. The free energy of the system is given by [14]

$$F=\int d\mathbf{r}[-a\psi^2+u\psi^4+d(\nabla\psi)^2+w(\nabla^2\psi)^2 +e\rho^2(\rho-\rho_s)^2-s\rho(\nabla\psi)^2], \tag{2.1}$$

where the parameters w, d, a, u, e, ρ_s, and s are all positive. The w and u terms ensure the thermodynamic stability of the system. The terms d and a are the usual Ginzburg-Landau free energy terms that disfavor creation of interfaces and disordered phases, respectively. The effect of d is counteracted by s: depending on the relative magnitudes of d and $s\rho(\mathbf{r},t)$, the creation of interfaces can be either energetically favorable or suppressed. The s term drives the surfactant to the interface between the two fluid components and the e term makes the surfactant density approach either zero (far away from interfaces) or ρ_s (near interfaces). Since in microemulsions the interface tension vanishes when the interface is saturated with surfactants [15], $d=s\rho_s$ will be chosen throughout this paper, so that creation of interfaces does not cost any energy when the local surfactant concentration is saturated, i.e., $\rho(\mathbf{r})=\rho_s$. The chemical potentials needed to ensure conservation of order parameters ψ and ρ have been omitted, because the kinetic equations considered below always place these constant terms under the action of spatial differentiation.

If the mixture is placed in a Hele-Shaw cell, its phase separation will be described by a set of kinetic equations [8],

$$\frac{\partial\psi(\mathbf{r},t)}{\partial t}+\mathbf{u}(\mathbf{r},t)\cdot\nabla\psi(\mathbf{r},t)=M_\psi\nabla^2\frac{\delta F}{\delta\psi(\mathbf{r},t)}+\eta_\psi(\mathbf{r},t), \tag{2.2a}$$

$$\frac{\partial\rho(\mathbf{r},t)}{\partial t}+\mathbf{u}(\mathbf{r},t)\cdot\nabla\rho(\mathbf{r},t)=M_\rho\nabla^2\frac{\delta F}{\delta\rho(\mathbf{r},t)}+\eta_\rho(\mathbf{r},t), \tag{2.2b}$$

$$\mathbf{u}=-\frac{1}{c^2}\left(\nabla p(\mathbf{r},t)-\frac{\delta F}{\delta\psi(\mathbf{r},t)}\nabla\psi(\mathbf{r},t)-\frac{\delta F}{\delta\rho(\mathbf{r},t)}\nabla\rho(\mathbf{r},t)\right). \tag{2.2c}$$

In Eqs. (2.2) M_ψ and M_ρ are transport coefficients and $\eta_\psi(\mathbf{r},t)$ and $\eta_\rho(\mathbf{r},t)$ are thermal fluctuations. The parameter $c^2>0$ measures the significance of hydrodynamic effects, which influence the system through the flow field $\mathbf{u}(\mathbf{r},t)$. The products $M_\psi c^2$ and $M_\rho c^2$ give the relative contributions of diffusive effects and hydrodynamic effects.

Simulations are implemented on an $L\times L$ square lattice $\mathbf{n}=(n_x,n_y)$ by using the the cell dynamic system (CDS) for fluids [16–18]:

$$\mathcal{I}(\mathbf{n},t)\equiv-A\tanh\psi(\mathbf{n},t)+\psi(\mathbf{n},t)+W(\tilde{\Delta})^2\psi(\mathbf{n},t) -(D-S\rho)\tilde{\Delta}\psi(\mathbf{n},t)+S\tilde{\nabla}\psi(\mathbf{n},t)\cdot\tilde{\nabla}\rho(\mathbf{n},t), \tag{2.3a}$$

$$\mathcal{J}(\mathbf{n},t)\equiv E\rho(\rho-\rho_s)(2\rho-\rho_s)-\tfrac{1}{2}S[\tilde{\nabla}\psi(\mathbf{n},t)]^2, \tag{2.3b}$$

$$\psi^*(\mathbf{n},t)\equiv\psi(\mathbf{n},t)+M_\psi\tilde{\Delta}\mathcal{I}(\mathbf{n},t)+C_\psi\eta_\psi(\mathbf{n},t), \tag{2.3c}$$

$$\rho^*(\mathbf{n},t)\equiv\rho(\mathbf{n},t)+M_\rho\tilde{\Delta}\mathcal{J}(\mathbf{n},t)+C_\rho\eta_\rho(\mathbf{n},t), \tag{2.3d}$$

$$p(\mathbf{n},t)=\mathcal{F}^{-1}\{[\nabla^2]_d^{-1}\mathcal{F}\tilde{\nabla}\cdot[\mathcal{I}(\mathbf{n},t)\tilde{\nabla}\psi(\mathbf{n},t) +\mathcal{J}(\mathbf{n},t)\tilde{\nabla}\rho(\mathbf{n},t)]\}, \tag{2.3e}$$

$$\mathbf{u}(\mathbf{n},t) = -\frac{1}{c^2}[\tilde{\nabla} p(\mathbf{n},t) - \mathcal{I}(\mathbf{n},t)\tilde{\nabla}\psi(\mathbf{n},t) - \mathcal{J}(\mathbf{n},t)\tilde{\nabla}\rho(\mathbf{n},t)], \tag{2.3f}$$

$$\psi(\mathbf{n},t+\Delta t) = \psi^*(\mathbf{n},t) - \tilde{\nabla}\cdot[\mathbf{u}(\mathbf{n},t)\psi^*(\mathbf{n},t)], \tag{2.3g}$$

$$\rho(\mathbf{n},t+\Delta t) = \rho^*(\mathbf{n},t) - \tilde{\nabla}\cdot[\mathbf{u}(\mathbf{n},t)\rho^*(\mathbf{n},t)], \tag{2.3h}$$

where $\mathcal{F}$ denotes the Fourier transform and Δt the time step size. The definitions for the CDS operators $\tilde{\nabla}$, $\tilde{\Delta}$, and $[\nabla^2]_d^{-1}$ can be found in Ref. [8]. The same CDS parameters as those in Ref. [8] are used: $L=128$, $A=1.3$, $W=0.2$, $D=0.5$, $S=0.5$, $E=0.25$, $\rho_s=1$, $M_\psi=M_\rho=0.05$, $c^2=10$, and $C_\psi=C_\rho=0.01$. The initial distributions used are also the same [8]: random uniform distributions between -0.01 and 0.01 (critical quench) for ψ and between $\langle\rho\rangle-0.01$ and $\langle\rho\rangle+0.01$ ($\langle\rho\rangle$ being the average surfactant concentration) for ρ. The values for c^2, C_ψ, and C_ρ are close to the maximum allowable values within the stability range of the CDS scheme.

III. RESULTS AND DISCUSSION

The number of time steps (i.e., number of iterations) in all simulations is 2.5×10^6. Five samples for $\langle\rho\rangle=0.25$, 0.35, 0.4, and 0.5 and two samples for $\langle\rho\rangle=0.2$ and 0.3 are used. Fewer samples are simulated for $\langle\rho\rangle=0.2$ and 0.3 because results for $\langle\rho\rangle=0.25$ and 0.35 show that for these low concentrations a single sample is already enough to reveal the characteristics of domain growth and the crossover [8,17,18]. In order to separate fluctuations introduced by initial configurations and by thermal fluctuations, the same set of samples are used for $\langle\rho\rangle=0.25$, 0.35, 0.4, and 0.5, and the first two of this set are used for $\langle\rho\rangle=0.2$ and 0.3.

A. Crossover

To assist the analysis of the simulation results, we first consider theoretically whether the crossover from the hydrodynamic regime to the thermal regime exists and its dependence on the surfactant concentration. We extend the analysis given in Ref. [8] and consider the Kawasaki-Ohta interface kinetic equation with thermal fluctuations [10],

$$\begin{aligned}\sigma K(a) - h(t)\Delta\psi_e = (\Delta\psi_e)^2 \int da' G(\mathbf{r}(a),\mathbf{r}(a'))v(a') \\ -(\Delta\psi_e)^2 \int da'da'' G(\mathbf{r}(a),\mathbf{r}(a'')) \\ \times \mathbf{n}(a')\cdot\mathbf{T}(\mathbf{r}(a'),\mathbf{r}(a''))\cdot\mathbf{n}(a'') \\ \times\sigma K(a'') + \theta(a,t),\end{aligned} \tag{3.1}$$

where σ denotes interface tension, $K(a)$ is the mean curvature at a, a point on the interface, and $h(t)$ is an auxiliary function to be determined by the conservation law. We will drop $h(t)$ in the following argument because we are only interested in the interplay between thermal fluctuations and hydrodynamics. $\Delta\psi_e$ is the difference between the two equilibrium ψ values. $v(a)$ gives the interface speed at a along $\mathbf{n}(a)$, the unit normal vector to the interface at a pointing from a domain with $\psi<0$ to an adjacent domain with $\psi>0$. $G(\mathbf{r},\mathbf{r}')$ is the Green's function that satisfies

$$M_\psi\nabla^2 G(\mathbf{r},\mathbf{r}') = -\delta(\mathbf{r}-\mathbf{r}') \tag{3.2}$$

under appropriate boundary conditions (determined by the geometry of a Hele-Shaw cell in our simulations). The thermal fluctuations $\theta(a,t)$ satisfy the following fluctuation-dissipation relation:

$$\begin{aligned}\langle\theta(a,t)\theta(a',t')\rangle \\ = 2k_BT(\Delta\psi_e)^2\delta(t-t')\Big(G(\mathbf{r}(a),\mathbf{r}(a')) + (\Delta\psi_e)^2 \\ \times\int da''d\tilde{a}\, G(\mathbf{r}(a),\mathbf{r}(a'')) \\ \times G(\mathbf{r}(a'),\mathbf{r}(\tilde{a}))\mathbf{n}(a'')\cdot\mathbf{T}(\mathbf{r}(a''),\mathbf{r}(\tilde{a}))\cdot\mathbf{n}(\tilde{a})\Big).\end{aligned} \tag{3.3}$$

$\mathbf{T}(\mathbf{r}(a),\mathbf{r}(a'))$ in Eqs. (3.1) and (3.3) is the Oseen tensor associated with Hele-Shaw geometry [8]. Equations (3.1), (3.2), and (3.3) give the following stochastic equation that dictates growth of the characteristic length scale $R(t)$:

$$\frac{d}{dt}R(t) \sim \sigma\left(M_\psi + \frac{\omega}{R(t)^2}\right) - M_\psi R(t)\theta(t), \tag{3.4a}$$

$$\langle\theta(t)\theta(t')\rangle \sim \frac{T}{M_\psi R(t)^2}\left(1+\frac{\omega}{M_\psi R(t)^2}\right), \tag{3.4b}$$

where ω is a measure of the hydrodynamic effects. Equation (3.4a) shows that the crossover occurs when the surface tension term is approximately equal to the thermal fluctuation term. When the hydrodynamic effect is strong, it gives

$$\sigma^2\omega \sim TR^2. \tag{3.5}$$

This equation shows that, consistent with intuition, thermal fluctuations will eventually overwhelm the coupled effect of hydrodynamics and interface tension as R gets greater and meanwhile σ gets smaller when the system evolves into the late stage.

The Kawasaki-Ohta equation, Eq. (3.1), assumes that the interface is infinitely sharp, so Eq. (3.5) can be applied only to the late stage of phase separation. However, we can extend its validity to a wider range by considering the physical meaning of the product $\sigma^2\omega$. This product is a measure of the joint effect of hydrodynamics and interface tension. In the very early stage, interface tension is large, but hydrodynamic convection is small, so their joint effect is small and thermal fluctuations dominate (Cahn-Hilliard-Cook regime). Once hydrodynamic convection is induced by interface motion, this joint effect dominates the system's evolution. Into the late stage, Eq. (3.5) applies, so thermal fluctuations will again dominate the system. Therefore, the left side of Eq. (3.5) can be schematically represented by a Gaussian-like curve, as shown in Fig. 1. Figure 1 shows that one can qualitatively solve Eq. (3.5) by considering the intersections of the two curves representing the thermal fluctuations and the joint effect of hydrodynamics and interface tension. These

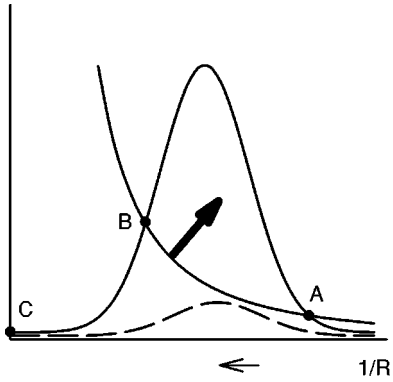

FIG. 1. Solution of Eq. (3.5) can be determined from the intersections of the joint effect of hydrodynamics and interface tension, represented by the Gaussian-like curve, and the thermal effect, represented by the hyperbolic curve. The system represented by the dashed Gaussian-like curve has higher surfactant concentration than the system represented by the solid Gaussian-like curve (see text). The solution A is the crossover from the thermal regime to the hydrodynamic regime at early times, whereas solution B is the second crossover back to the thermal regime. When temperature is increased, the hyperbola moves outward, as indicated by the bold arrow, narrowing the interval in $1/R$ (and, therefore, in time) between the two crossovers. The thin arrow indicates the direction of phase separation. Point C is a measure of the joint effect of hydrodynamics and interface tension at a very late stage. It is expected to be very small. Combining this with the fact that this joint effect is also small in the very early stage, a Gaussian-like curve serves as a qualitative estimation of the joint effect.

intersections show that, in general, there should exist two crossovers, one (A in Fig. 1) for the first crossover from the thermal regime to the hydrodynamic regime and one (B in Fig. 1) for the second crossover back to thermal regime. To see how surfactant concentration affects these crossovers, consider two systems, one with high surfactant concentration and the other with low surfactant concentration. At the same characteristic length scale, $\sigma^2\omega$ for the system with high surfactant concentration is expected to be smaller because the interfaces can be covered by surfactants more completely (especially at the late stage) and slower evolution makes convection less significant. Therefore, the curve representing the $\sigma^2\omega$ term (the dashed curve in Fig. 1) should lie beneath that for the system with low surfactant concentration. It can be seen from Fig. 1 that at higher surfactant concentrations, the two crossovers A and B will get closer and eventually disappear, namely, thermal fluctuations will dominate the system at all times if the surfactant concentration is higher than a critical concentration. Therefore, the interval in $1/R$ in which hydrodynamics dominates is expected to be shorter when surfactant concentration increases. (This does not imply that it will take a shorter time for systems with high surfactant concentration to reach the crossover. These systems evolve more slowly, compared with systems with lower surfactant concentration, so whether this is the case also depends on the rate at which $1/R$ goes from A to B.)

Now let us turn to simulation results. Figure 2 shows the domain growth for individual samples at each surfactant concentration. While the transition at which the system becomes more susceptible to thermal fluctuations is rather discernible at $\langle\rho\rangle=0.35$ and 0.4, it is not clear whether this transition exists at $\langle\rho\rangle=0.25$ and 0.5. However, observations based on individual samples can be illusory and we shall demonstrate below that the ensemble average suggests that the growth at $\langle\rho\rangle=0.25$ is still dominated by hydrodynamics regardless of the (accidental) great fluctuations over samples. The growth of average domain size for surfactant concentrations $\langle\rho\rangle=0.25$, 0.35, 0.4, and 0.5 is shown in Fig. 3. The figures display the behavior of ensembles of various size. An individual sample's behavior can be roughly inferred by comparing the growth curves of ensembles whose sizes differ by one sample [19]. Figure 4 summarizes all the domain growth curves. (See Ref. [8] for the definition of the inverse characteristic length scale $\langle k_\psi\rangle$ used here.) For all surfactant concentrations, an intermediate stage where the growth curve exhibits a definite slope, regardless of the number of samples included, can easily be discerned. This easily discernible slope is a sign that the system is dominated by a deterministic driving force—hydrodynamics. This in turn implies that none of the systems simulated has surfactant concentration high enough to allow thermal fluctuations to be dominant at all times. Into the late stage, the growth curve for systems with lower surfactant concentrations shows a sudden change in slope and those for systems with higher surfactant concentrations exhibit the onset of growing fluctuations. The slope change and the onset of growing fluctuations suggest that the system has crossed the crossover and is no longer entirely dominated by hydrodynamics. At lower surfactant concentrations, regardless of the number of samples included in the average, one can still see a clear growth slope in the late stage, implying that hydrodynamics is still substantially responsible for the domain growth. On the other hand, at higher surfactant concentrations, it becomes more difficult to see the slope in the late stage. This suggests that the thermal fluctuations have already significantly overwhelmed hydrodynamics. Thus, systems with higher surfactant concentration do appear to have a smaller interval in $\langle k\rangle$ where hydrodynamics dominates (the corresponding interval in time, accidentally, is also shorter).

Figure 5 shows the fluctuation [(standard deviation)/$\|$mean$\|$] in $\log_{10}\langle k_\psi\rangle$. [Note that this figure is *not* directly obtained from Figs. 3(b)—3(d) because that would bias the distribution to the first few samples. The method used is explained in the figure's caption.] Although one of the samples of the system with $\langle\rho\rangle=0.25$ accidentally suffers great fluctuations in the intermediate stage, the remaining deterministic, hydrodynamic influence eventually averages it out and decreases the fluctuation to the lowest level of all the systems. The system with $\langle\rho\rangle=0.35$ is also able to keep the fluctuation at a relatively low level. The slowly varying fluctuation seen at the late stage is consistent with the fact that a clear growth slope exists in the late stage for $\langle\rho\rangle=0.25$ and 0.35. On the other hand, systems with higher surfactant concentrations, $\langle\rho\rangle=0.4$ and 0.5, show significant growing fluctuations, making determining the growth slope very difficult.

Because the crossover may not be very sharp, it is more difficult to locate the crossover and determine its dependence on surfactant concentration more quantitatively. At low surfactant concentrations, since the growth curve still shows anunambiguous constant slope in the late stage, the crossover can be located by fitting the data [20] that are away from, before and after, the crossover separately and finding the

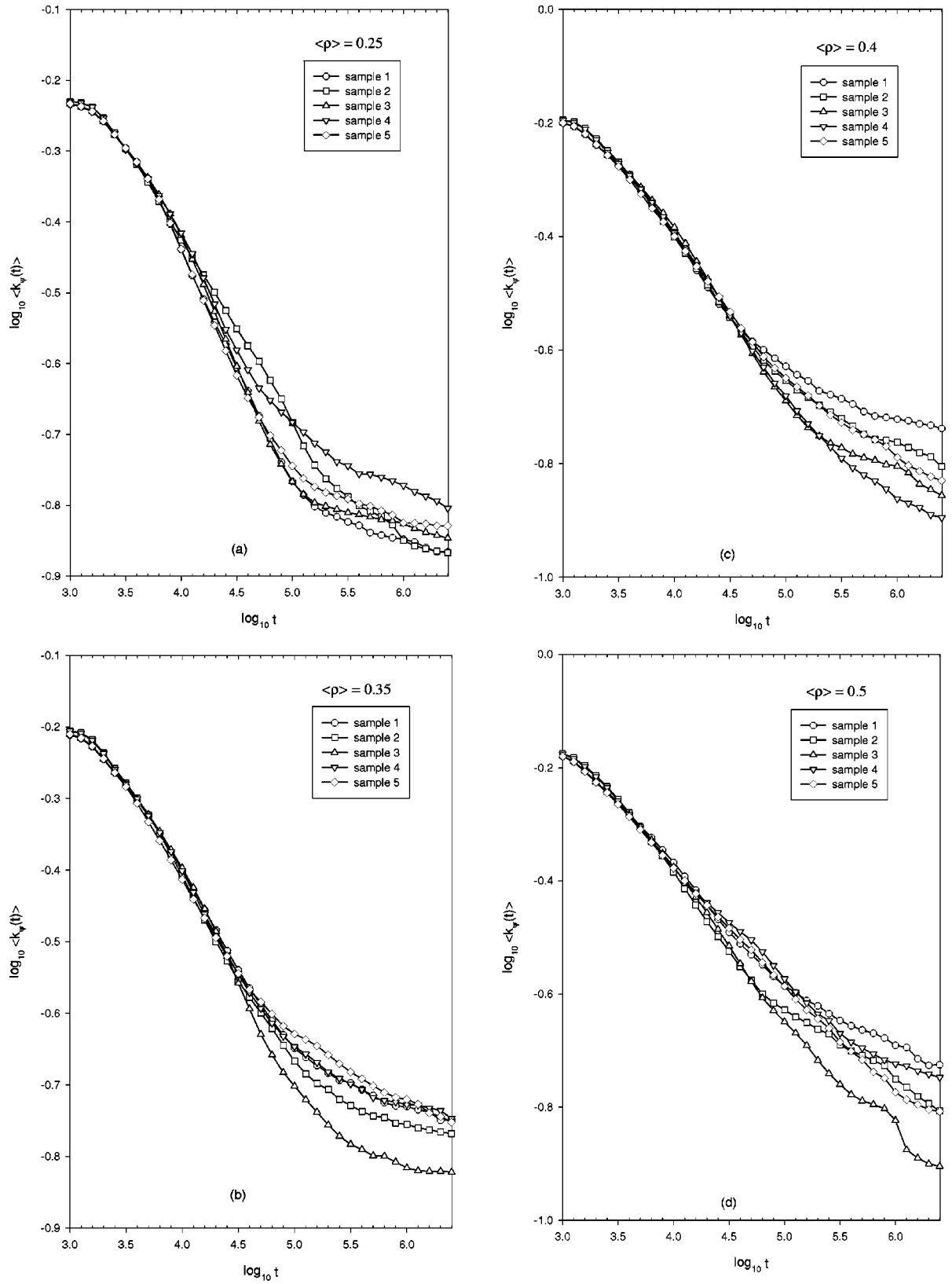

FIG. 2. The inverse characteristic length scale as a function of time steps for (a) $\langle\rho\rangle=0.25$, (b) $\langle\rho\rangle=0.35$, (c) $\langle\rho\rangle=0.4$, and (d) $\langle\rho\rangle=0.5$.

intersection of the two optimal curves. As noted above, hydrodynamics has not been completely overwhelmed in the late stage in these systems; what is located by this method is expected to be an estimate of the crossover's lower bound. At higher surfactant concentrations, this method does not apply because it is difficult to determine the slope of the growth curve. Alternatively, fluctuations in the growth curve over the ensemble (for example, Fig. 5) may be used. How-

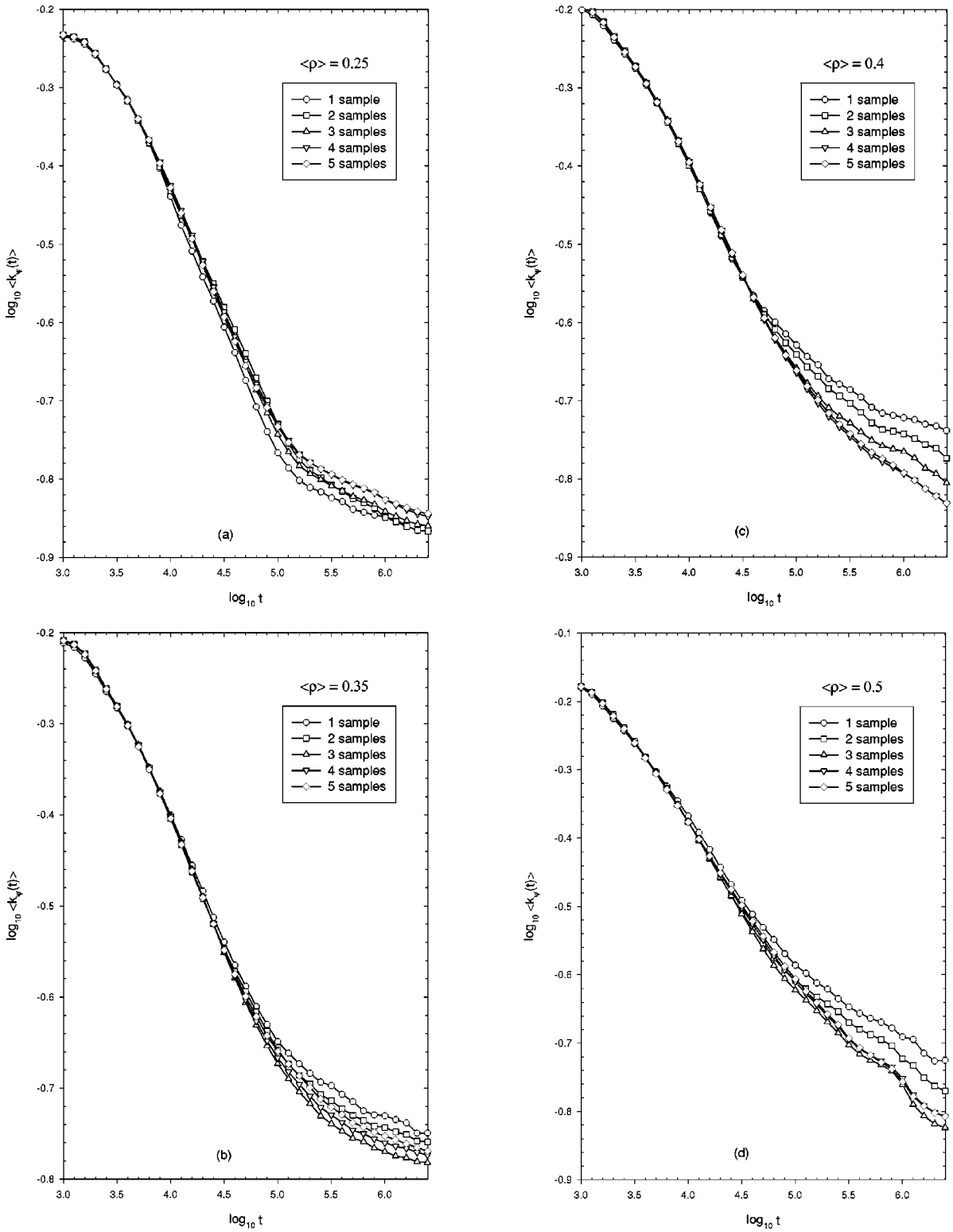

FIG. 3. The inverse characteristic length scale as a function of time steps. (a) $\langle\rho\rangle = 0.25$. Domain growth shows a clear crossover around $t = 10^{5.15}$. It can be seen that including more samples in the ensemble has very little effect on the general shape of the growth curve. (b) $\langle\rho\rangle = 0.35$. Compared with (a) the crossover is less clear and data beyond the crossover show more significant fluctuations. (c) $\langle\rho\rangle = 0.4$. (d) $\langle\rho\rangle = 0.5$.

ever, because the crossover is probably not very sharp and, even if it is sharply defined, to quantitatively and unambiguously locate it requires more samples in the ensemble, these two methods cannot unequivocally locate the crossover [21].

B. Trapping of surfactants

Reference [8] has demonstrated that surfactants are likely to be trapped in domains when the system has high fluidity and has surfactant concentration that is higher than a thresh-

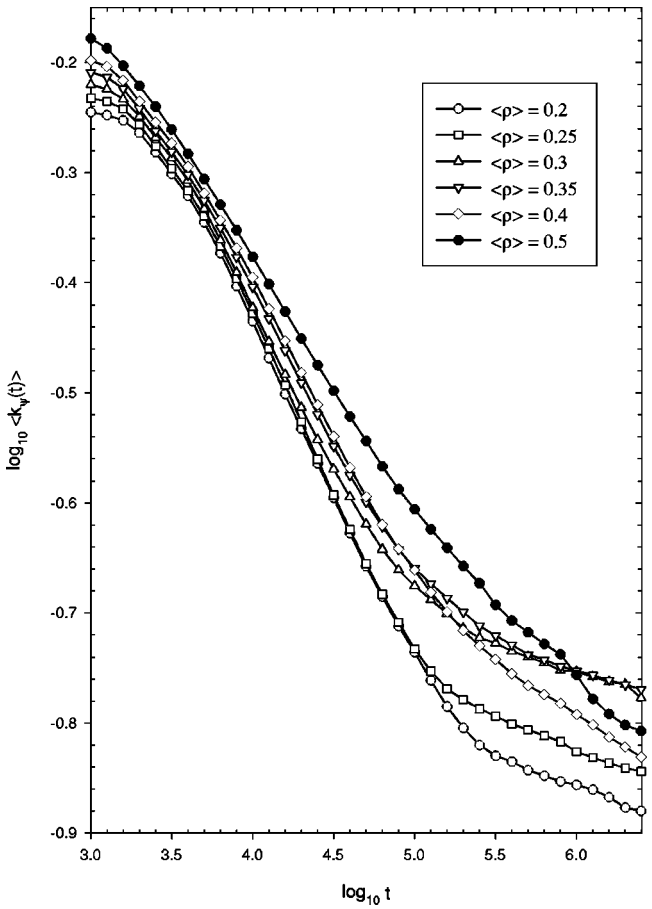

FIG. 4. The inverse characteristic length scale as a function of time steps for different average surfactant concentrations. Curves for $\langle\rho\rangle=0.2$ and 0.3 are obtained from two samples. All the others are obtained from five samples.

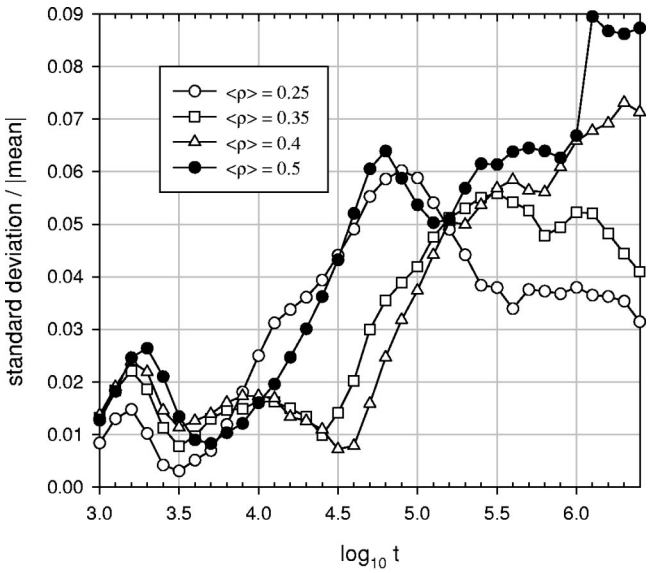

FIG. 5. Variation of the dispersion in the inverse characteristic length scale $\langle k_\psi\rangle$. This figure is obtained by first calculating $\langle k_\psi\rangle$ for each sample at each time. The standard deviation is then obtained from all the samples with the same surfactant concentration at each time.

old $\langle\rho\rangle_c$. An explanation for this phenomenon was given in Ref. [8]. There it was shown that, although it is also theoretically possible to trap the surfactants in domains when hydrodynamic effects are absent, trapping is realized in practice only when the motion of domain boundaries is accelerated by hydrodynamics. The absence of this phenomenon in systems without hydrodynamic effects suggests that trapping is not due to micelle formation, further confirming the important role of hydrodynamics. However, to observe this trapping phenomenon in real systems, one cannot ignore thermal fluctuations. Since thermal fluctuations and the induced convection help the trapped surfactants diffuse, the trapping phenomenon may soon disappear. It is therefore necessary to investigate how effective thermal fluctuations are in removing trapped surfactants. A preliminary simulation, with the largest possible thermal fluctuations included, performed in Ref. [8] was not long enough to give a crude estimation for the lifetime scale of the trapping phenomenon. Our more extensive simulations here, which are five times longer, still see no sign of the complete escape of the trapped surfactants (though some do succeed in finding their ways to the interfaces, as expected) when the fluidity takes the maximum possible value [8]. Surfactants are seen trapped up to the end of the simulation ($t=2.5\times10^6$) in all samples at $\langle\rho\rangle=0.3$, 0.35, 0.4, and 0.5. Three of the five samples at $\langle\rho\rangle=0.25$ show trapped surfactants, but only one sample is able to keep them trapped till the end of the simulation. (The threshold concentration $\langle\rho\rangle_c$ above which trapping can be observed has been estimated to be slightly larger than 0.2 [8]. Simulations carried out here confirm this estimation.) These results suggest that the trapped surfactants in systems having high surfactant concentrations, for example, $\langle\rho\rangle=0.4$ and 0.5, can be very long lived, compared with the time the system needed to achieve well-separated domains. (Domains are already well separated at $t\approx5\times10^4$, so the lifetimes of the trapped surfactants can easily reach a few hundred times this time scale.) Since the orientations of surfactant molecules are not included in the model used here, the configurations of the trapped surfactants are not specified. The trapped surfactants presumably can form micelles. This suggests that formation of micelles may be enhanced by phase separation of the host solution.

While thermal fluctuations help decrease the amount of surfactants trapped, on the other hand, trapped surfactants can also be created by thermal fluctuations even in the late stage. It is expected that the presence of surfactants will eventually stop the domain growth. The stopping of growth can be seen in systems without thermal fluctuations, whether hydrodynamic effects exist or not, as demonstrated in Fig. 17 of Ref. [8]. When there are thermal fluctuations, as shown here in Fig. 4, it will take a time much longer than our simulation to see the end of growth. This is because thermal fluctuations help the length scale grow by shuffling the surfactants at the interfaces and evaporating small domains. The latter process can create new trapped surfactants in the late stage. Figure 6 shows an example. This figure is taken from the third sample in Fig. 2(d). While the domains change rather little from $t=5\times10^5$ ($=10^{5.7}$) to $t=1\times10^6$ (the biggest change being the slight withdrawal of the peninsula labeled by *A*), there are significant changes (evaporation of small domains) from $t=1\times10^6$ to $t=1.6\times10^6$ ($=10^{6.2}$). [These changes are responsible for the sudden drop from t

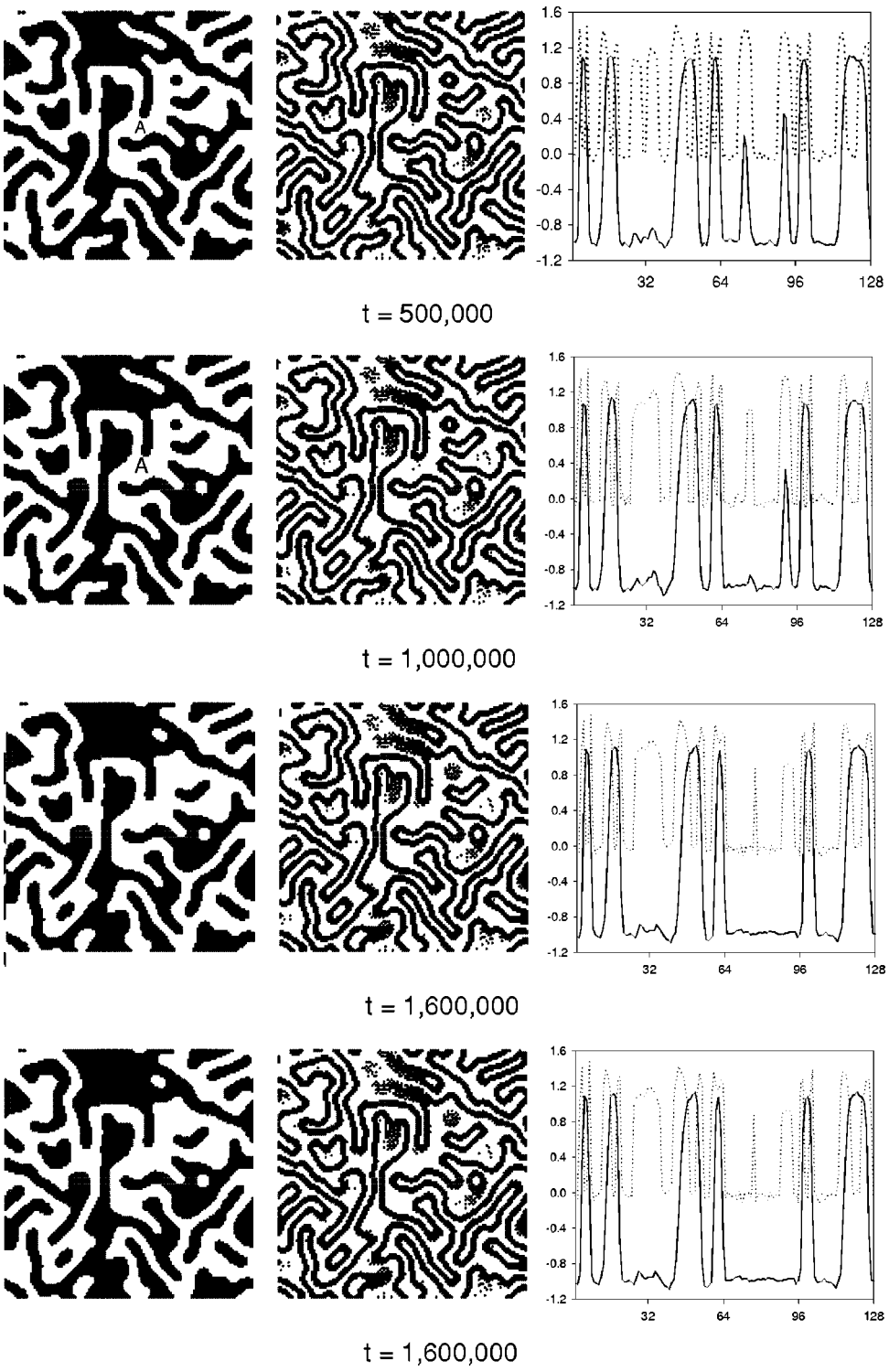

FIG. 6. Time evolution of binary fluid domains (left), surfactants (middle), and their density profile (solid line for the binary fluid and dotted line for the surfactants) along the [1,1] direction (right) in late stage. $\langle\rho\rangle=0.5$. The peninsula marked by *A* withdraws a little from $t=5\times10^5$ to $t=1\times10^6$. This withdrawal eliminates the smaller peak (solid line) seen around cell 96 in the corresponding profile plots. The main changes from $t=1\times10^6$ to $t=1.6\times10^6$ are the complete evaporation of a circular island and the shrinking of a slender island to a small ellipse in the upper part of the system. Careful inspection of the density profile reveals that the foot of the peak (solid line) to the right of cell 32 never stops moving to the right, indicating that thermal fluctuations keep sharpening the interfaces. This interface sharpening is not discernible in the ''hardened'' system [18] displayed by the plots in the left and middle columns.

$=10^6$ to $t=10^{6.1}$ in Fig. 3(d).] Newly trapped surfactants can be seen at the places where domains have evaporated.

We do not know of any experimental evidence for this trapping phenomenon. One possible way to observe it experimentally is to bring the system away from the quasiequilibrium state that it achieves at late times. Then the trapped surfactants may become nucleation sites that can be observed. Note that, according to the argument given in Ref. [8], the specific form of the model free energy used, Eq. (2.1), is not responsible for the trapping of surfactants. It is expected that, as long as the equations of motion are given by Eqs. (2.2), any model free energy should be capable of displaying this phenomenon. Dimensionality and boundary conditions may change the specific form of Eq. (2.2c); however, these will not change the conclusion provided the velocity field is slaved.

IV. CONCLUSION

We have shown that there exists a crossover from the hydrodynamic regime to the thermal fluctuation regime in a phase-separating binary fluid/surfactant system. The cross-

over depends on the average surfactant concentration, and increasing surfactant concentration brings the crossover to an earlier time. As the surfactant concentration increases, this crossover will move closer to the first crossover where the system crosses from the Cahn-Hilliard-Cook regime to the hydrodynamic regime. There should exist a critical concentration above which thermal fluctuations overwhelm hydrodynamics at all times. Simulations confirm the existence of the crossover and, qualitatively, its dependence on the concentration of surfactants. Simulations also show that surfactants can be trapped in domains for a very long time, much longer than the time needed for the binary fluid too become well segregated. It is therefore possible to observe this trapping phenomenon (as far as its lifetime is concerned; real systems may not have the high fluidity needed to trap surfactants) and formation of micelles may be enhanced by this phenomenon. The trapped surfactants may also serve as nucleation sites when the system undergoes a second quench.

The analytical arguments given in Sec. III A for the crossover and in Ref. [8] for trapping are based on a general equation, Eq. (3.1), which is applicable when the binary fluid has been well segregated, and on a set of general kinetic equations, Eqs. (2.2). Therefore, models based on a Ginzburg-Landau free energy other than Eq. (2.1) are expected to be able to display the same crossover and trapping found in the current model. Since the arguments do not rely on the system's composition, we believe that the condition $\langle \psi \rangle = 0$ (critical quench) is not essential for the existence of the crossover and the trapping phenomenon. Finally, neither dimensionality nor boundary conditions changes the arguments substantially, so it should be straightforward to generalize them to other two-dimensional systems with different flow fields, such as Langmuir monolayers [22] and three-dimensional systems.

ACKNOWLEDGMENT

This work was supported in part by the National Science Council of the Republic of China (Taiwan) under Contract No. NSC-89-2112-M-001-005.

[1] See A. J. Bray, Adv. Phys. **43**, 357 (1994), and references therein.

[2] Recently, M. Grant and K. R. Elder [Phys. Rev. Lett. **82**, 14 (1999)] argued that the finiteness of the Reynolds number gives an upper bound for the growth exponent, $\alpha \leqslant 1/2$, in the asymptotic regime. Therefore, there should exist yet another crossover that has not been observed in simulations that reported greater values.

[3] See, for example, S. Puri and N. Parekh, J. Phys. A **25**, 4127 (1992).

[4] T. Kawakatsu, K. Kawasaki, M. Furusaka, H. Okabayashi, and T. Kanaya, J. Phys.: Condens. Matter **6**, 6385 (1994), and references therein.

[5] D. Chowdhury, J. Phys.: Condens. Matter **6**, 2435 (1994), and references therein.

[6] R. Ahluwalia and S. Puri, J. Phys.: Condens. Matter **8**, 227 (1996), and references therein.

[7] H. Tanaka and T. Araki [Phys. Rev. Lett. **81**, 389 (1998)] reported that dynamic scaling could not be observed under high-fluidity. It is not clear how much the free boundary condition used, which in two dimensions leads to a fictitious hydrodynamic interaction that varies with logarithmically spatial separation, is responsible for this result. It is interesting to note that H. Chen and A. Chakrabarti, [J. Chem. Phys. **108**, 6006 (1998)] used this divergent hydrodynamic interaction and obtained results that look ''normal.''

[8] J.-R. Roan and E. I. Shakhnovich, Phys. Rev. E **59**, 2109 (1999).

[9] The estimation of surface tension used in Ref. [8] may seem pathological. It was based on the following consideration. The amount of surfactants at the interfaces is expected to be roughly proportional to $\langle \rho \rangle$. ρR can serve as a measure of this amount, so $\rho R \propto \langle \rho \rangle$. This estimation of course breaks down in the early stage, which was not the concern of Ref. [8].

[10] K. Kawasaki and T. Ohta, Physica A **118**, 175 (1983).

[11] G. Gompper and M. Schick, *Self-Assembling Amphiphilic Systems* (Academic Press, London, 1994), and references therein.

[12] G. Pätzold and K. Dawson, Phys. Rev. E **52**, 6908 (1995).

[13] Reference [12] also includes all these three effects in some simulations. However, there is no mention of the trapped surfactants and the function of thermal fluctuations is to keep the domain structures from being frozen prematurely (which is also observed in Ref. [8]).

[14] S. Komura and H. Kodama, Phys. Rev. E **55**, 1722 (1997).

[15] P.-G. de Gennes and C. Taupin, J. Phys. Chem. **86**, 2294 (1982).

[16] Y. Oono and S. Puri, Phys. Rev. Lett. **58**, 836 (1987); Phys. Rev. A **38**, 434 (1988).

[17] A. Shinozaki and Y. Oono, Phys. Rev. A **45**, R2161 (1992).

[18] A. Shinozaki and Y. Oono, Phys. Rev. E **48**, 2622 (1993).

[19] Figures 3(c) and 3(d) may suggest to some readers that there is a systematic drift when more samples are included. This is, however, not the case. As stated in the text, an individual sample's growth curve can be roughly retrieved. The reader can then see that there is no systematic drift that drives the growth curve downward.

[20] In Ref. [8] it is shown that logarithmic growth laws and algebraic growth laws work equally well because the true growth law is far more complicated and contains many parameters. Both can be used to fit the data.

[21] The two methods are complementary. When two slopes can be clearly seen in the growth curve regardless of the number of samples included, there is no point in using the other method. When the second slope cannot be unambiguously determined for all ensembles, using the slopes to locate the crossover is not reliable. We find the borderline between these two methods is around $\langle \rho \rangle = 0.35$. The locations of the crossover determined at different $\langle \rho \rangle$ are consistent with the theoretical expectation given in Sec. III A. However, the crossover is probably not sharp and what these methods give is an estimation of the lower bound and the upper bound, respectively, so it is difficult to make an unequivocal quantitative analysis.

[22] H. A. Stone and H. M. McConnell, Proc. R. Soc. London, Ser. A **448**, 97 (1995).